Adv. Space Res. Vol.4, No.2-3, pp.157-160, 1984
Printed in Great Britain.

0273-1177/84 $0.00 + .50

ACCELERATION OF PARTICLES IN SHOCKED MAGNETIC NEUTRAL SHEETS

D. J. Mullan,* J. Perez-Peraza,** M. Galvez** and M. Alvarez**

**Bartol Research Foundation, University of Delaware, Newark, DE 19716, U.S.A.*
***Instituto De Geofisica, UNAM, 04510 Mexico 20 DF, Mexico*

ABSTRACT

We report on a study of particle acceleration in a magnetic neutral sheet which has been struck by a passing MHD shock, such as occurs in the sun when a flare occurs near a helmet streamer. Using trajectory calculations, we derive energy spectra. We propose that long-lived particle events with energies up to 10-100 MeV following solar flares may be explained by the mechanism described here.

1. INTRODUCTION

Collapsing magnetic neutral sheets (CMNS) are widely considered as sites of particle acceleration, especially at the heart of a solar flare /1/, where rapid energy release ensures (or is caused by) violent collapse near an X-type neutral point. CMNS may also be useful for "quiescent" coronal heating /2/. Here we consider an intermediate case: a large coronal neutral sheet (e.g. in a helmet streamer), initially in a state of essentially static equilibrium, and hence of little interest for particle acceleration. But if a flare occurs nearby, it may create an MHD shock which eventually sweeps over the neutral sheet. The likelihood of such an event is high, since a helmet streamer probably exists within a few tens of heliographic degrees of many solar flares /3/. Here we ask: Can a shocked helmet streamer act as a source of particles with characteristics corresponding to an observed component of solar energetic particles In Section 2, we describe a simulation of the shock-neutral sheet interaction. In Sections 3-5 we describe how we compute particle energy spectra in the neutral sheet. We compare our spectra with those of long-lived solar particle events.

2. SIMULATION OF SHOCK INTERACTION WITH NEUTRAL SHEET

The neutral sheet in a helmet streamer extends essentially radially above the solar surface. Our simulation in the meridional plane is shown in Fig. 1. Our 2-D MHD code is described in /3/: the 60 x 60 computational grid extends from $\theta = 90^\circ$ to 105° and over a radial distance from r=1 (solar surface) to r=1.3. At t=0, a pressure pulse is introduced at the position $r = 1, \theta = 90^\circ$, to simulate a flare on the solar surface some distance away from the base of the "helmet streamer". The "flare" (which is sustained at a constant amplitude for a finite time) creates an MHD shock which sweeps out across the grid, eventually reaching the base of the neutral sheet, and interacting with the neutral sheet at progressively greater heights as time goes on. The computation is stopped at a time (t = 5 min.) when the disturbance reaches the boundary of the grid. In the earlier work /3/, the major interest was in how the neutral sheet affected the shock. Here, we are interested in how the shock affects the neutral sheet. For the present work, the output which we need from the simulation consists of the physical conditions throughout the grid at t = 5 min., i.e. velocities, temperatures, and magnetic field strengths (B) at all points of our 60 x 60 grid. With these, we start our particle trajectory calculations.

3. DELINEATION OF ACCELERATION REGION

Particle acceleration in a neutral sheet depends on the existence of an electric field $E \neq 0$ in the region where $B \approx 0$. The electric field induced by the diffusion of the plasma across the magnetic field is $E = -(\underline{V}_d \times \underline{B})/c$ where V_d is the drift velocity of plasma relative to the magnetic field lines. In the present context, it is not possible to use the steady-state thickness of the diffusion region since, with the recent passage of a shock front, there is no guarantee that a steady state has been achieved. For that reason, we have developed two approximate methods of identifying the diffusion region.

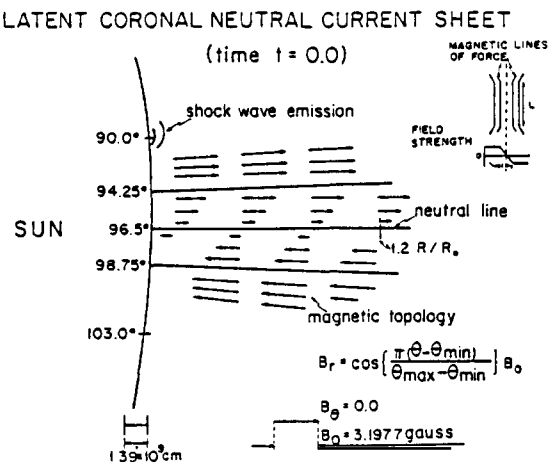

Fig. 1

Fig. 2

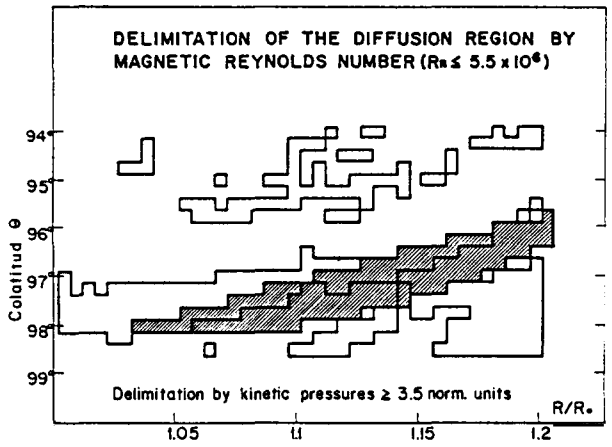

Fig. 3(a)

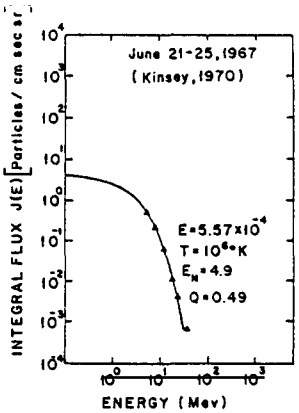

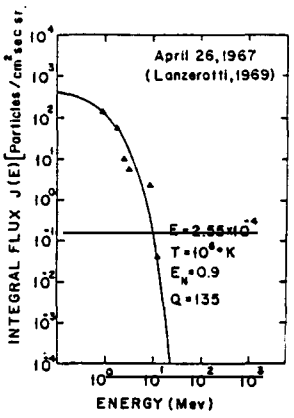

Fig. 3(b)

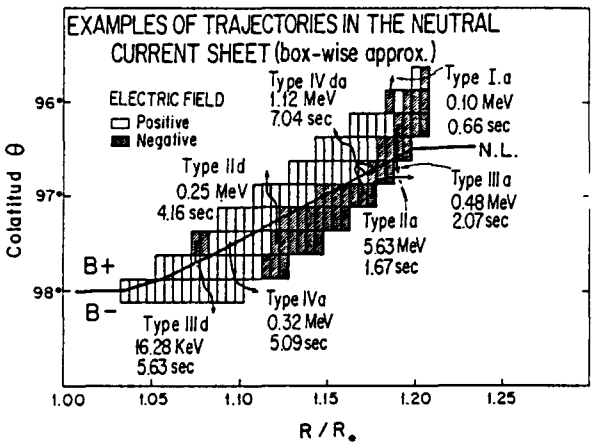

Fig. 4

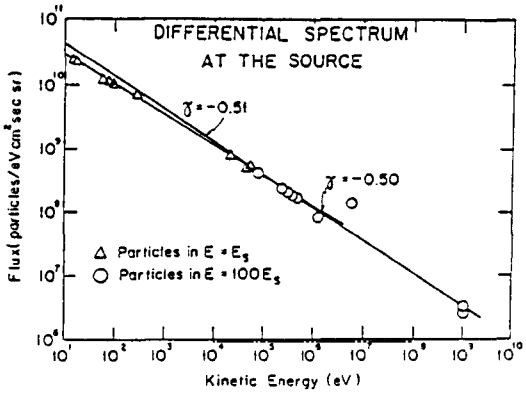

Fig. 5

First, we argue from the overall dynamics of the shock interaction: an MHD shock is focussed into a neutral sheet, forcing the sheet to collapse more rapidly, and causing enhanced local dissipation /3/, in the form of enhanced gas pressures. We choose the region of maximum gas pressures ($P > P_{crit}$) as an indication of the region of maximum dissipation, and correspondingly, the region of most rapid collapse. We selected $P_{crit} = 3.5$ P (initial). The diffusion region delineated according to this criterion is shown (shaded) in Figure 2.

As a second method of delineating the diffusion region, we consider the local values of the magnetic reynolds number, $R_m = \text{curl } (v \times B)/(\eta \nabla^2 B)$ (where η is magnetic diffusivity). In the undisturbed corona, this quantity is very large, indicating that the flux and plasma are frozen effectively together. But in the diffusion region, R_m decreases. We therefore use the criterion $R_m < R_m$ (crit) in order to define the diffusion region. In evaluating R_m we use the anomalous electrical conductivity, because the neutral sheet has recently been compressed by the passing shock: such compression in general leads to plasma turbulence, where the electrical conductivity $\sigma = 1.5 \times 10^6 N^{1/2}$ c.g.s. can be as much as 10^6 times less than the Spitzer value /4/. We evaluate R_m at each point of our grid by numerical differentiation of the simulation variables at t=5 min. Selecting R_m (crit) = 5.5×10^6 ~ (100 times lower than the typical value in the quiet corona), we find a diffusion region in the vicinity of the shocked neutral sheet as shown (unshaded) in Figure 2. Although not identifical with the diffusion region delineated by the pressure criterion, we consider that the overlap in the two regions in quite good. We will for definiteness choose the shaded diffusion region in what follows.

Particle acceleration occurs entirely inside the diffusion region shown in Fig. 2. Notice that the shape of the diffusion region is no longer perpendicular to the solar surface (as the initial neutral sheet was). The shock has displaced the base of the neutral sheet, but has not yet had time to interact with the topmost layers of the sheet. The diffusion region, with the imbedded neutral line makes an angle $\phi = 8.45^\circ$ with respect to the radial direction at t = 5 m. Hence, if the local components of flow velocity are V_r and V_θ, the velocity component perpendicular to the neutral sheet at t = 5 min. is $V_r \sin\phi + V_\theta \cos\phi$. Our 2-D MHD code gives no information about the thickness of the diffusion region perpendicular to the r-θ plane. We have arbitrarily assigned a thickness of the same order of magnitude as the width of the diffusion region in Fig. 2.

4. PARTICLE ACCELERATION: ZEROTH ORDER

The diffusion region occupies 112 "boxes" in our computational grid. To evaluate the local E-field we assigned a unique flow velocity to each box. The magnetic field in the vicinity of the simulated neutral sheet was fitted to a continuous topology of X-type form: $B_x = B_0 P y$, $B_y = B_0 K x$ where $B_0 = 3.1977$ Gauss, and P = 21 and K = 0.7 were chosen to represent as well as possible the simulated field at t = 5 min. (Notice that, in order to derive these quantities, we approximated the r-θ grid by a cartesian system oriented along the neutral line.) With this approach, the electric fields in the various boxes of the diffusion region were found to lie in the range 10^{-6} - 10^{-2} c.g.s.

If we could assign a unique E-field to all the boxes, then the energy spectrum of the accelerated particles would be analytic /5/:

$$N(\varepsilon) \propto (\varepsilon/\varepsilon_0)^{-1/4} \exp(-1.12(\varepsilon/\varepsilon_0)^{1/4}) \quad (1)$$

where the cut-off energy ε_0 depends on the E-field according to $\varepsilon_0 = A E^{4/3}$, and the parameter A depends on the magnetic field gradient close to the X-type neutral line, $A \propto 1/(B_0 P)^2$. The spectra of long-lived solar particle events have been reported in /6/ and /7/. Their energy spectra are shown in Fig. 3 along with attempts to fit the observed spectra with curves of the form in eq. (1). The key parameter in fitting each spectrum is ε_0, i.e., E. The fits shown in the figure require us to choose E in the range (2-6) x 10^{-4} c.g.s. We note that these electric fields overlap with the range of local electric field values which emerged in our simulation. We stress that the simulation had been performed with no reference whatsoever to solar particle acceleration: in the simulation, parameter choices were guided solely by the properties of coronal helmet streamers and flare shocks. Thus, there is in principle no reason to expect that the simulation E-fields would have any bearing on the E-fields required to explain the observed spectra. We regard this zeroth order result as an encouraging sign that shocked helmet streamers may explain the particles reported in /6/ and /7/.

If our explanation is correct, the "turn-on" time and duration of such a source of solar particles would be determined by coronal propagation time-scales. With coronal velocities of 100-1000 km/sec, and flare separations of up to 60 degrees (heliographic) from the nearest helmet streamer, the time lapse between flare and "turn-on" of the helmet streamer source would range from 10 minutes to a couple of hours. Similarly, the duration of the source, assuming streamer lengths in the range from 1 to 10 solar radii,

would range from 10 minutes to almost one day. Hence we consider this mechanism to be a viable source of the long-lived components. Of course, the assumption of a unique and uniform electric field throughout the acceleration region is a gross simplification of the actual conditions in the vicinity of the neutral sheet.

5. PARTICLE ACCELERATION: TRAJECTORIES

In view of the encouraging results reported above, we have advanced to the next higher approximation, and calculated trajectories of individual particles in the 112 boxes of the diffusion region. To compute these trajectories, we adopted the continuous magnetic topology mentioned above. In each box, the plasma flow was assumed to be uniform, but with the magnetic field varying continuously, the induced electric field also varied continuously across each box. Turbulent fluctuations in the flow will certainly lead to local deviations of E from the gross average: these derivations may play a key role in particle acceleration /8/. Our electric field is "boxwise" continuous.

In each box, we evaluated V_d (which enters into E) as the difference between the local flow velocity in that box and the overall velocity of the neutral line itself. Thus, in box "i", the drift velocity is $V_d = V_i - V_0$, where V_0 is the vector velocity of the neutral line itself. At $\theta < 96^\circ.5$ (Fig. 1) compression of the sheet corresponds to $V_d>0$ (since V_i consists mainly of a θ-component), whereas at $\theta>96^\circ.5$, compression corresponds to $V_d<0$. Boxes in which compression is still occurring at t = 5 min. (and where particle acceleration is maximally efficient) are denoted as shaded boxes in Fig. 4. Particles which spend most of their trajectory in "favorable" boxes are labelled "a" in Fig. 4. On the other hand, boxes which were shocked at times $t << 5$ min. are now in a state of relaxation following shock passage, and they are expanding (unshaded boxes in Fig. 4). Particles are decelerated in such boxes (see label "d" on certain particles in Fig. 4).

The trajectory calculation begins with injection of a thermal particle in a box, and the trajectory is followed until the particle leaves the diffusion region altogether. To build a spectrum, we assume that all of the gas particles which were originally in a particular "box" will experience the same acceleration. In this way, we build up the energy spectrum shown in Figure 5. The trajectories were performed not only with the E-field predicted by the simulation ($E = \alpha E_S$, α=1), but also with $\alpha = 100$. By this method, we allow crudely for large localized fluctuations in the E-field. We find a power law spectrum, falling off rather slowly, as $E^{-0.5}$ over the energy range from 10 eV to >100 MeV. Thus, we confirm one of the conclusions of the zeroth order approach, namely, a shocked helmet streamer can create particles with energies of many MeV. The spectral index is almost independent of α, but the maximum energy increases rapidly with α. Because of the great range in E-fields in the various simulation boxes (10^{-6}-10^{-2} c.g.s., if α=1), the spectral cut-off ϵ_0 which occurs in the case of uniform E is not apparent. The great range in E-fields in the simulation boxes is partly attributable to numerical fluctuations (especially in differencing the velocity vectors of local flow relative to the neutral line flow). In the real sun, the E-fields might span a narrower range: if so, the spectrum is Fig. 5 would be compressed into a narrower energy range, with an upper cut-off.

6. CONCLUSIONS

We have described two methods to calculate the energy spectrum of particles which are accelerated in a shocked neutral sheet in the solar corona. The first approach is analytic, but it requires oversimplifying the electric field structure in the neutral sheet. The second approach involves the numerical integration of particle trajectories in the vicinity of the neutral sheet. Both approaches lead to essentially the same conclusion: if a coronal helmet streamer is "hit" by a flare-induced MHD shock wave, the streamer will act as a source of 10-100 MeV particles. We propose this as a source of long-lived solar particle events, which create particles up to the above energies for periods of some hours after a flare.

We acknowledge support from CONACYT and NSF for this work.

REFERENCES

1. R.Giovanelli, Mon. Not. Roy. Astron. Soc. 107, 338 (1947).
2. R.H. Levine, Ap.J. 192, 457 (1974).
3. R.S. Steinolfson and D.J. Mullan, Ap.J. 241, 1186 (1980).
4. J. Heyvaerts and M. Kuperus, Astron. Ap. 64, 219 (1978).
5. J. Perez-Peraza, et al, Proc. 15th ICRC 5, 23 (1977).
6. J.H. Kinsey, Phys. Rev. Letters 24, 246 (1970).
7. L.J. Lanzerotti, J. Geophys. Res. 74, 2851 (1969).
8. W.H. Matthaeus, in preparation (1984).